Machine Learning Approaches forto Debris Flow Susceptibility

2 Analyses in the Yunnan section of the Nujiang River Basin

- 3 Jingyi Zhou¹, Jiangcheng Huang², Zhengbao Sun³, Qi Yi¹, Aoyang He²
- 4 ¹ School of Earth Sciences, Yunnan University, Kunming, Yunnan Province, China
- 5 Institute of International Rivers and Eco-Security, Yunnan University, Kunming, Yunnan Province, China
 - ³ School of Engineering, Yunnan University, Kunming, Yunnan Province, China
- 8 Corresponding Author:
- 9 Qi Yi¹

6

7

11

- 10 Wujiaying Street, Kunming, Yunnan Province, 650500, China
- 12 Email address: yiqi1018@126.com

Commentato [MR1]: General comment: the manuscript, with a few exceptions, cites predominantly impacted chinese literature. This is not necessarily a problem particularlty when discussing study area and problems therein, but limits the analysis and its generalizibility to a small Chinese context. I kindly suggest to give a more broad international context to the analysis, adding and analysing international citation/references.

3 Machine Learning Approaches forto Debris Flow

14 Susceptibility Analyses in the Yunnan section of the Nujiang

15 River Basin

16 17

18 Jingyi Zhou¹, Jiangcheng Huang², Zhengbao Sun³, Qi Yi¹, Aoyang He²

19

- 20 ¹ School of Earth Sciences, Yunnan University, Kunming, Yunnan Province, China;
- 21 ² Institute of International Rivers and Eco-Security, Yunnan University, Kunming, Yunnan
- 22 Province, China;
- 23 School of Engineering, Yunnan University, Kunming, Yunnan Province, China;

24

29

33

39

- 25 Corresponding Author:
- 26 Qi Yi¹
- 27 Wujiaying Street, Kunming, Yunnan Province, 650500, China
- 28 Email address: yiqi1018@126.com

30 Abstract

- 31 **Background.** The Yunnan section of the Nujiang River (YNR) Basin aerossin the alpine-valley
- 32 area is one of the most critical areas of debris flow in China.
 - Methods. To assess the susceptibility of alpine-valley area debris flows and explore the
- 34 assessment methods, we selected 20 factors to compare and analyze We analyzed the applicability
- of three machine learning algorithms forto modeling, namely, of susceptibility to debris flow -
- 36 the random forest (RF), the linear kernel support vector machine (Linear SVM), and the radial
- basis function support vector machine (RBFSVM), and dissected compared 20 factors to
- 38 determine the dominant factors of ones in debris flow occurrence in the region.
 - Results. The results show We found that (1) the RF, which is more suitable for the DFS research,
- 40 outperforms the outperformed RBFSVM and Linear SVM in terms of accuracy—, (2) In YNR
- 41 Basin, topographic conditions are prerequisites determined, and the regional setting combination
- 42 of geology, precipitation, vegetation, and anthropogenic influence play a crucial role in was
- 43 <u>critical to forming debris flows.</u> In addition Also, the relative elevation difference is found to
- 44 bewas the most prominent evaluation factor, followed by the watershed area, among 20 factors.

ha formattato: Tipo di carattere: Times New Roman

Commentato [MR2]: Substitute with "model"

Commentato [MR3]: Substitute with " - "

Commentato [MR4]: Substitute with "controlling"

ha formattato: Tipo di carattere: Times New Roman

Commentato [MR5]: Check sentence grammar and structure

(3) Susceptibility of debris flow susceptibility, and (3) susceptibility maps based on RF's DFS showdebris flow susceptibility (DFS) showed that zones with very high susceptibility zones are were distributed along the mainstream of the Nujiang River in the study area, and are mostly located in counties such as Gongshan, Fugong, and Lushui. The These findings of this study can provide underlying techniques for alpine valley area debris flow assessment methodological guidance and reference for improvement of DFS assessment. It enriches the content of DFS studies in the alpine-valley areas.

Keywords

debris flow susceptibility, random forest model, support vector machine, Nujiang River, alpinevalley-area

Introduction

Debris flow is a natural disaster widely distributed characterized by water and sand movement occurring frequently in countries areas around the world with special terrain and geomorphic conditions. The process of water and sand accumulation is very complex and is influenced by various natural and human factors.

The Yunnan section of the Nujiang River (YNR) Basin, located in the transitional zone between China's first and second terraces, is the core of the Kunlun-Qinling Mountains, is the southwestcenter of southwestern longitudinal ridges and valleys. It has huge undulations in the ridge and valley area. The terrain is undulating with a relative elevation difference of over 4700 m (Tang, 2005; Xu, 2016). This region frequently experiences prolonged and intense precipitation during the rainy seasonseasons, increasing the moisture content in the area of the rocky and unconsolidated sediment (Ming, 2006a). Under Debris flows form under the surface hydrodynamic action, debris flows seriously and imperil the lives and property locally. According to literature statistics of the local population.

On average, there has been are 8 debris flows per 10 km² on average in the YNR Basin, which is one of the world'sworld's most severe debris flow areas (*Tang*, 2005; *Yang et al.*, 2017), which is one of the world'sworld's most severe debris flow areas (*Tang*, 2005; *Yang et al.*, 2017), Based A total of 283 debris flows occurred in the basin from 1999 to 2008, based on the geological hazard investigation and zoning records of Yunnan Province spanning from 1999 to 2008, a total of 283 debris flows occurred in the basin. On the In two specific incidents alone, hugemassive debris flows happenedoccurred in Gongshan County on July 26 and August 18, 2010 and resulted resulting in nearly 100 deaths and hundreds of millions of yuan Yuan in economic losses (*Min et al.*, 2013). It is critical to clarify the spatiotemporal correlation between debris flows and driving factors, as well as to scientifically predict the debris flow susceptibility

Commentato [MR6]: This description is too basic and partly erroneous. Indeed debris flows may involve not only sandy material. Please correct and refer to existing literature

Formattato: Rientro: Prima riga: 0,74 cm

Commentato [MR7]: In China?

ha formattato: Tipo di carattere: Times New Roman

Commentato [MR8]: Substitute with "events"

(DFS) in YNR Basin.

Generally, research on the DFS assessment method can be divided into heuristic, physical modelling, and data driven approaches (Chang et al., 2019; Dou et al., 2019; Reichenbach et al., 2018; Sun et al., 2021; Zhou et al., 2020). Traditional research work was dominated by heuristic approaches, which were quite time-consuming and costly, unsuitable for large-scale promotion and application. In addition, the study results lack comparability due to non-uniform metrics (Dou et al., 2019; Huang et al., 2022). Physical models are mainly used to simulate the mechanism of debris flow movement and make predictions. For example, a shallow water model based on the finite volume method to predict the potential magnitude of debris flows, which can accurately and efficiently solve the fluid flow problem in irregular terrain (Bao et al., 2019). Nevertheless, the processes of model building are complex and with high expense, which is fulfilling to assess the susceptibility of single-gully debris flows, rather than larger regions (Luo & Liu, 2018). Other conventional methods such as fuzzy logic (Li et al., 2017), hierarchical analysis (LiouNguyen & Li, 2017), and network analysis (Sujatha & Sridhar, 2017) have some defects in revealing the spatial distribution pattern of non-linearity. With the rapid development of artificial intelligence methods and techniques, emerging data-driven approaches have been widely adopted in large scale study areas, such as support vector machine (Chang et al., 2019), random forest model (Liang et al., 2020), and convolutional neural network (Zhang et al., 2019) owing to their higher accuracy and more precise prediction results (Oh & Lee, 2017).

Up to now, although lots of researches have discussed the relative merits in terms of the accuracy and prediction results of various models in different study areas, there are few comparative research on susceptibility models and driving factors of alpine-valley area debris flow (*Liang et al.*, 2020; *Zhang et al.*, 2019). Besides, current models have been developed and designed mainly for specific application needs of a certain research area, lacking a uniform general model (*Lana Castro & Lana*, 2022; *Reichenbach et al.*, 2018).

To explore a research model applicable to the alpine valley typologies on account of A clear understanding of the spatiotemporal relationships between debris flows and their evolution factors holds profound implications for society. Firstly, authorities and residents will be able to implement targeted preventive measures by effectively identifying and assessing potential debris flow risk areas, significantly enhancing society's overall preparedness and ultimately reducing casualties and property losses. Secondly, accurate susceptibility analysis will help avoid construction in potentially hazardous debris flow areas, while spatiotemporal correlation analysis will aid planners in assessing potential impact areas and frequency of debris flows. This will contribute to reducing the impact of disasters on urban infrastructure and enhancing overall

resilience of cities. Further, understanding of the spatiotemporal relationships between debris flows and their evolution factors will facilitate more efficient allocation of resources. The proactive deployment of emergency rescue resources ensures a swift and organized response in an event of a disaster, minimizing the overall impact. Additionally, susceptibility analysis serves as the foundation for establishing an effective early warning system. Through monitoring potential debris flow risk areas, timely identification of signs of potential debris flows, and rapid issuance of warnings, residents can take appropriate preventive and evacuation measures, thus maximizing the reduction of casualties. Finally, an in-depth spatiotemporal correlation analysis aids scientists in gaining a better understanding of the formation mechanisms and evolutionary patterns of debris flows, providing a more accurate foundation for risk management (*Janizadeh et al.*, 2019).

Table 1: Classification of DFS assessment methods.

Despite numerous studies addressing the accuracy of various models and the relative merits of predictive outcomes for different areas (Table 1), comparative research on susceptibility and evaluation factors of debris flows in alpine-valley areas is limited. The scarcity can be attributed to the challenging nature of collecting data in these remote regions, which are characterized by limited transportation, poor road conditions, and inherent difficulties of accessing high mountainous terrain. Additionally, existing studies often rely on conventional debris flow susceptibility assessment methods, which exhibit lower accuracy and fail to meet practical requirements (*Liang et al.*, 2020; *Zhang et al.*, 2019).

To enhance the accuracy and precision of DFS assessment, in alpine-valley areas and to research vitalexplore the key factors in the influencing debris flow formation of debris flows and DFS classificationalong with the spatial distribution map in YNR Basinof debris flow classifications, we tried to construct and compare DFS assessment models based on random forestcollected debris flow data from satellite images, vector images, raster images, reports, papers, books, and statistical data, and verified them with local records and data driven approaches that can effectively integrate multiple sources and capture the nonlinear and complex relationships among them. We then constructed DFS models based on Random Forest (RF), radial basis function support vector machine Radial Basis Function Support Vector Machine (RBFSVM), and linear kernel support vector machine Linear Kernel Support Vector Machine (Linear SVM) in YNR Basin.). The model models yielded accuracy, prediction predictive performance, and prediction results were obtained and used as evaluation metrics for models' applicability, looking forward to provide the underlying techniques for enriching the research means of outcome assessments. This study provides methodological guidance and reference for

ha formattato: Colore carattere: Automatico

Formattato: Regola lo spazio tra testo asiatico e in alfabeto latino, Regola lo spazio tra caratteri asiatici e numeri

ha formattato: Colore carattere: Automatico

Commentato [MR9]: Unclear, please specify

the improvement of DFS assessment and improves the accuracy of susceptibility studies of debris flows in alpine-valley area debris flow. This study is of practical significance to enrich the study of alpine-valley area debris flows and to facilitate the debris flow disaster reduction areas. It also contributes to the enhancement of disaster mitigation and prevention planning in urban and rural areas of the YNR Basin.

Commentato [MR10]: These seem more conclusions than introductory sentences

Study area

The YNR Basin, between 23°07′ 28°23′N and 98°07′ 100°30′E, spanning approximately 30000 km², is located in the longitudinal ridges and valleys belt of western Yunnan Province (Fig. between 23°07′–28°23′N and 98°07′–100°30′E covering approximately 30 000 km² (Fig. 1), and); the area is at the southeastern edge of the strong extrusion zone between the Asian and European plates and the Indian Ocean plate, with strong geological and tectonic movements (*Ma*, 1999). The geomorphological development is controlled by the deep and large fractures of the Nujiang River, and debris flows are distributed in bands along the fracture zones and gullies (*GuoLuo & Tang*, 2015). This section is located in the southwest monsoon area with distinct wet and dry features (*Guo*, *Luo* & *Tang*, 2015). Study area is located in the southwest monsoon area with distinct wet and dry periods, and the rainy season is concentrated from April to September (*Ming*, 2006b).

Considering differences in topography and vegetation cover in the study area, the The YNR basin was used to be divided into the upstream and the downstream section by the boundary between Lushui County and Longyang District considering differences in topography and vegetation cover in the study area (Xu, 2016)(Xu, 2016). The upstream area is of has a typical alpine-valley landscape characterized by high mountains, deep valleys, steep slopes, and swiftly flowing water (Huang et al., 2020a). Where There are the Gaoligong mountain range and, the Gawa Gap, the Bilo and Meri snow mountains tower aloft, the The relative height difference reaches 3000m. 3000 m between the highest and lowest points of the study area. The Nujiang River, is extremely long and narrow, runs through in these large mountains, with a maximum basin width of 267 km and a narrowest of only 21 km. The downstream has relatively flat terrain on both sides, with many hills and alluvia alluvia fans of uneven sizes. The vegetation

<u>Vegetation</u> cover of the Yunnan section of the Nujiang River Basin is relatively high, with dominant dry-hot river valley shrub-grassland flanking both sides of the valley. The <u>vegetation Vegetation</u> types change in order as from an evergreen forest, semi-evergreen forest, deciduous forest, mixed broad-leaved coniferous forest, coniferous forest, and alpine shrubs from valleys to ridges (*Luo*, 2009; Xu, 2016). (*Luo*, 2009; Xu, 2016). The majority of soil types are red-

yellow soils with loose texture, poor erosion resistance, and water retention in the basin, and shift in the order of the red loam, the yellow-red loam, the yellow-brown loam, the brown loam, the dark brown loam, the grey-brown forest soil, and the alpine meadow soil along with the rising elevation rising (Liu, 2017). With the rapid

Rapid socio-economic development, of the area accelerates the changes in geologic environment due to human activities such as town and rural built-land expansion, steep slope cultivation, road construction, and mining engineering further accelerate changes in the geological environment. According to the literature, Literature indicates that the Nujiang River basin is the most serious geological hazard among the 6 major basins in Yunnan Province, especially upstream of the YNR Basin (*Huang et al.*, 2020b; Tang & Zhu, 2003).

Fig. 1: YNR basin (Study area).

Methods and data

3.1 Research Methodology

The overall method flow is shown in Fig. 2.

Fig. 2: Research methodology. (a) General procedure. (b) Detailed procedure of the methods construction in the general procedure.

3.1.1 The Random forest model

The random forest model is an integrated algorithm consisting of multiple unrelated decision trees, where the final output is determined by all decision trees in the forest together, which was The random forest model is effective in capturing and simulating complex nonlinear relationships between debris flows and evaluation factors, and can handle large-scale, high-dimensional debris flow datasets without overfitting. Furthermore, the RF indicates the relative importance of each evaluation factor, guiding the understanding of which factors have the greatest impact on debris flow susceptibility. It also demonstrates good adaptability to noise and outliers in the data, making it less susceptible to interference. Therefore, RF exhibits excellent applicability to assessments of debris flow susceptibility(Duan et al., 2022; Zhang & Wu, 2019).

The RF is an integrated algorithm consisting of multiple unrelated decision trees that determine the DFS, in which the final output is determined by all decision trees together, and is defined as (*Breiman*, 2001),

Commentato [MR11]: remove

Commentato [MR12]: Unclear, please rephrase

Formattato: Rientro: Prima riga: 0,74 cm

$$H(x) = \arg \max_{Z} \sum_{i=1}^{k} I(h_i(x) = Z)$$
 (1)

where H(x) denotes the model output results of the model's predicted DFS for each watershed unit, $h_i(x)$ denotes atthe *i*th decision tree, *x* denotes attributes, $h_i(x) = Z$ is the prediction of variable *Z* using the *i*th tree in variable *x*, and $I(\cdot)$ is the prediction of each decision tree.

Given a database, the RF can be interpreted via the 3-following three steps: Firstly, sample subsets are extracted using the Bootstrap resampling method. In other wordsSpecifically, n sample subsets of the same size as the original sample are extracted using the put-back method. Secondly, construct a decision tree is constructed for each sample subset. Among the attributes of the sample subset, k attributes are randomly selected. Then, select the best partitioning attributes of the nodes between decision trees are selected based on the Gini Index, which wasis calculated

$$Gini(p) = \sum_{k=1}^{k} p_k (1 - p_k) = 1 - \sum_{k=1}^{k} p_k^2$$
 (2)

where p_k indicates the probability that the selected sample belongs to category k. The smallerSmaller Gini Index meansIndexes mean that the probability of a selected sample in the set being misclassified is smaller. Finally, n decision trees are combined to generate a random forest-(Fig. 3).

Fig. 3: The Process of the RF model.

Hyperparameters of the RF model can be divided into two categories: those that determine the sampling method, such as bootstrap and the number of classifiers that determine the sampling method, and the number of decision trees, respectively. And those, Parameters that determine the decision tree, such as maximum depth (max_depth,-), minimum number of samples for a leaf node (min_samples_leaf,-), minimum number of samples required to split an internal node (min_samples_split,-), the maximum number of features randomly selected as candidates for splitting (max_features,), and a_criterion that determinedetermines the maximum depth, minimum number of samples for a leaf node, minimum number of samples required to split an internal node, the maximum number of features randomly selected as candidates for splitting, and a_criterion for the optimal split attribute.

3.1.2 The Support vector machine

The Support Vector Machine (SVM) demonstrates superior classification performance on unseen data due to its outstanding generalization capability, laying a crucial foundation for the credibility

Commentato [MR13]: In the end of the formula there is a symbol to be removed

Formattato: Rientro: Prima riga: 0,74 cm

and practicality of the model in real-world applications. In practical applications, areas prone to debris flows encompass complex environmental features, and SVM's excellent handling of high-dimensional data provides robust support for assessing susceptibility considering multiple evaluation factors. Additionally, by employing various kernel functions, SVM exhibits flexibility in modeling nonlinear relationships in high-dimensional space, thereby enhancing its applicability in the assessment of DFS. These attributes position SVM as a powerful tool when facing real and complex datasets, providing a reliable analytical framework for accurately evaluating DFS.

There are two cases of linearly divisible and linearly indivisible sample data in the feature space. The basic principle of SVM is to find the optimal classification hyperplane for two types (Fig. 4). As an example of binary data, a binary classification space $D(X_i, Y_i)$, $i = 1, ..., l. X_i \in R_n, Y_i \in \{1, -1\}$, where, l represents the number of samples, and n denotes input dimensionality. The hyperplane $\omega x + b = 0$ can be found in the original space when the sample data are linearly divisible, separating the two classes of samples completely. When the sample data is are linearly indivisible, the input space it is necessary to perform nonlinear mapping $\Phi(x)$, mapping it from the input space to a certain feature space, the classification hyperplane can be expressed as $\omega \Phi(x) + b = 0$; meantime, the optimal hyperplane that requires $2/\|\omega\|$ is the largest, and the problem is transformed into a high-dimensional feature space through a non-quadratic programming problem, with the application of the Lagrange multiplier method for the solution, namely,

$$\begin{cases} \min \frac{\|\omega\|^2}{2} + C \sum_{i=1}^{l} \varepsilon_i, \\ s.t. y_i(\omega \cdot x_i + b) \ge 1 - \varepsilon_i, \\ \varepsilon_i \ge 0, i = 1, 2, \dots, l \end{cases}$$
(3)

where ε_i is the slack variable and C is the penalty factor. According to the Kuhn-Tucker (K-T) condition, the following dyadic problem can be obtained:

$$\max \sum_{i=1}^{l} a_{i} - \frac{1}{2} \sum_{i=1}^{l} \sum_{j=1}^{l} a_{i} a_{j} y_{i} y_{j} \varphi(x_{i}) \cdot \varphi(x_{j}),$$

$$s. t. \ 0 \le a_{i} \le C, \sum_{i=1}^{l} a_{i} y_{i} = 0$$
(4)

By solving the dyadic problem of this quadratic programming, the discriminant function is obtained as:

267
$$f(x) = sign \sum_{i=1}^{l} a_i y_i [\Phi(x_i) \cdot \Phi(x_j)] + b$$
 (5)

According to the relevant theory of generalized functions, as long as a kind of kernel function $K(x_i, y_i)$ satisfies the Mercer condition, it corresponds to an inner product in a certain transformed space, $K(x_i, y_i) = \Phi(x_i) \cdot \Phi(x_j)$, and linear classification of a certain nonlinear transformation defined be achieved by the using a different inner product function. Then a linear judgment function is constructed in this high dimensional feature space to find the optimal classification hyperplane, achieving linearly divisible datasurface (Suykens & Vandewalle, 1999).

Linear Kernel, Polynomial Kernel, Sigmoid Kernel, and the Radial Basis Function (RBF) are commonly used in support vector machine models, where,

Linear Kernel

$$K(y, y^{\star}) = y^{T} y^{\star} \tag{3}$$

$$K(y, y') = y^T y' (6)$$

279 RBF

$$K(y, y^{t}) = \exp\left(\frac{1}{2\sigma^{2}} \|y - y^{t}\|^{2}\right) \tag{4}$$

$$K(y, y') = \exp\left(-\frac{1}{2\sigma^2} \|y - y'\|^2\right)$$
 (7)

where y and y' are both basis vectors in the feature space, and σ is a model's hyperparameter. Compared with the Linear Kernel, Thethe RBF can transform the features² dimensionality for reducing the computational complexity, which is extremely suitable for predicting DFS in high-dimensional feature spaces (Lin & Lin, 2003). The penalty parameter C, an empirical parameter in the SVM model, is employedused to control the tolerance of systematic outliers, allowing for a few outliers to exist in the opponent classification. A higher value of the penalty parameter leads to fewer outliers in the opponent classification. What's more, the radial basis function kernel has an additional kernel parameter γ i.e., kernel bandwidth to be optimized, where $\gamma = 1/2\sigma^2$. As γ increases, the fit changes towards non-linear.

Fig. 4: Support vector machine models. (a) Linearly divisible case. (b) Linearly indivisible case.

3.1.3 Accuracy evaluation metrics

Evaluation of model's accuracy is critical for decision-makers and relevant institutions. High-precision model predictions contribute to more precise decision-making, ensuring that measures taken are scientifically sound and effective. Comparing the accuracy of different models in practical applications contributes to the selection of the most suitable model for a given region or

Formattato: Rientro: Prima riga: 0,74 cm

topography, thereby bolstering the credibility of predictions. Additionally, accuracy evaluation provides feedback on the current model performance, guiding continuous improvement efforts.

298

299

300

301

302

303

304

305

306

307

308

309

310

311

312

313

314

315

316

317

318

319

323

324

325

326

Accuracy, Precision, Recall, Kappa, F1-score, Receiver Operating Characteristics Characteristic (ROC) curve, and Area Under ROC (AUC) are employed used as the accuracy evaluation metrics. Accuracy indicates represents the proportion of correctly classified debris flow samples-, serving as a key indicator for overall model performance. Precision refers to the proportion of the samples with positive cases that are correctly predictedwhich are critical for reducing false positives and ensuring the rational use of limited resources. Recall indicates the proportion of positive cases that are correctly predicted in the true sample-The, and is essential for minimizing the risk of overlooking potential hazard zones. F1-score is used for the overall evaluation of Precision and Recall, and the offers a balanced assessment of precision and recall, guiding the establishment of reasonable warning and management strategies. A higher the value, the higher the F1-score indicates greater model accuracy. Kappa measures the model consistency. The larger, indicating its ability to make similar judgments under different conditions or at different times. In the value, the higher the context of dynamic changes in debris flow risk, model stability is essential for providing continuous and effective risk assessments. A higher Kappa means greater classification accuracy. The ROC curve is generated aids decisionmakers in balancing sensitivity and specificity by using True Positive Rate (TPR) as the vertical axis and False Positive Rate (FPR) as the horizontal axis. The AUC is obtained by integrating the ROC curve and, reflects the model's classification effect of the model. The value of effectiveness Even in situations with imbalanced positive and negative samples, a higher AUC is closer to 1,

 $\frac{TP + TN}{Accuracy} = \frac{TP + TN}{TP + FP + FN + TN}$

the more accurate the value indicates superior model isaccuracy. Their definitions are as follows,

 $\frac{Precission = \frac{TP}{TP + FP}}{Recall = \frac{TP}{TP + FN}}$

 $\frac{F1}{F1} \frac{score}{score} = \frac{2 * Precission * Recall}{Precission + Recall}$ $\frac{Kappa}{1 - p_x} = \frac{1 - p_x}{(9)}$

 $\frac{p_e}{TP + FP * (TP + FN) + (FN + TN) * (FP + TN)}{(TP + FP + FN + TN) * (TP + FP + FN + TN)} \tag{10}$

TP

 $Accuracy = \frac{TP + TN}{TP + FP + FN + TN} \tag{8}$

ha formattato: Tipo di carattere: Corsivo

Formattato: Rientro: Prima riga: 0,74 cm

ha formattato: Tipo di carattere: Corsivo

ha formattato: Tipo di carattere: Non Corsivo

ha formattato: Tipo di carattere: Corsivo

$$Precission = \frac{TP}{TP + FP} \tag{9}$$

$$Recall = \frac{TP}{TP + FN} \tag{10}$$

$$F1 - score = \frac{2 * Precision * Recall}{Precision + Recall}$$
 (11)

330

331

332

333

334

335

336

337

338

339

340

341

342

343

344

345 346

347

348

349

350

351

352

353

354

$$F1 - score = \frac{2 * Precision * Recall}{Precision + Recall}$$

$$Kappa = \frac{Accuracy - p_e}{1 - p_e}$$
(11)

$$p_e = \frac{(TP + FP) * (TP + FN) + (FN + TN) * (FP + TN)}{(TP + FP + FN + TN) * (TP + FP + FN + TN)}$$
(13)

The ROC curve is generated using the True Positive Rate (TPR) as the vertical axis and False Positive Rate (FPR) as the horizontal axis. The AUC is obtained by integrating the ROC curve and it reflects the classification effect of the model. The closer its value is to 1, the better and more accurate the model is. The calculation is as follows,

$$\frac{TPR = \frac{TP}{TP + FN}}{FPR = \frac{FP}{FP + TN}} \tag{11}$$

$$\frac{FPR = \frac{FP}{FP + TN}}{(12)}$$

$$TPR = \frac{TP}{TP + FN} \tag{14}$$

$$FPR = \frac{FP}{FP + TN} \tag{15}$$

where in Equations 5-128-15, TP standstands for the true positive rate, FP represents the false positive rate, TN signifies the true negative rate, and FN denotes the false negative rate.

Equal spacing, equal quantile, and natural breakpoint methods are the most widely used methods of data discretization To facilitate horizontal comparisons of model predictions, many studies use the equal spacing method to classify DFS into five zones and confirm the method's applicability (Liang et al., 2020; Liu, Miao & Tian, 2017). Therefore, in this study, we divided the predicted debris flow susceptibility calculated by the three models into five classes, from low to high, corresponding to the very low susceptibility zones (0 to <0.2), low susceptibility zones (0.2 to <0.4), medium susceptibility zones (0.4 to <0.6), high susceptibility zones (0.6 to <0.8) and very high susceptibility zones (0.8 to <1), respectively (Zhang & Wu, 2019). To facilitate horizontal comparisons of model predictions, many studies use the equal spacing method to classify DFS into five zones and confirm the method's applicability (Liang et al., 2020; LiuMiao & Tian, 2017). Therefore, in this study, we divide the predicted susceptibility of the three models into five classes at a constant interval scale, from low to high, corresponding to the very low susceptibility zones (0-0.2), the low susceptibility zones (0.2-0.4), the medium susceptibility

355 zones (0.4-0.6), the high susceptibility zones (0.6-0.8) and the very high susceptibility zones 356 (0.8-1), respectively. 357 3.2 Data and processing 358 3.2.1 Evaluation units 359 Raster cells and watershed units in DEM are commonly used for susceptibility 360 assessments (Zou et al., 2017). Raster cells are more convenient for modelling and 361 calculation because of their regular shape and uniform size, while watershed units can represent 362 integrated geomorphological characteristics of hydrological processes, and that helpholps in 363 obtaining the actual conditions of debris flow (Liu et al., 2018; Qiang et al., 2019; Zhang et al., 364 2022). Therefore, we adopted watershed units as the basic evaluation units and used ArcMap's 365 hydrological analysis tools to categorize the 30 m spatial resolution DEM data of the YNR Basin. 366 Finally, the study area was divided into 1070 watershed units. 367 3.2.2 Evaluation factors 368 The formation of debris flows is determined by a combination of factors (*Huang et al.*, 369 2022). (Huang et al., 2022). After conducting a thorough investigation, data collection, and 370 preliminary analysis of existing data on the historical background, geological structure, 371 topography and geomorphology, hydro-meteorology, soil and vegetation, and human activities in 372 the study area, we selected evaluation factors from five aspects: topographic conditions, rainfall 373 conditions, geological-conditions, and vegetation conditions, and human activities-(Table 2). 374 (1) Topographic conditions. Topographic conditions play a crucial role in are critical to the 375 formation of debris flows. Drawing on the results of others' research (Liu & Tang, 1995; Sun et 376 al., 2021), weWe chose relative elevation difference and slope to represent the potential energy of 377 watersheds and the ability to carry the rocky soil, respectively, and selected the watershed area to 378 reflect the for runoff and sediment yield-calculations based on previous research in this area by 379 (Liu & Tang, 1995; Sun et al., 2021). Therefore, based on the DEM with a spatial resolution of 30 380 meters, the mean relative elevation difference and average slope of each watershed unit had

beenwere calculated using the ArcMap function of zonal statistics as a table, and the area of each

(2) Rainfall conditions. Rainfall is necessary for debris flow incubating and triggering

Earlier Antecedent rainfall serves mainly serves to wet or soften the soil and reduce the stability

of rocky soil. Short-duration heavy rainfall brings rainfalls create a strong mechanical impact on

the soil that is about to be saturated or almost saturated, and disrupts disrupt the equilibrium of the

watershed unit had been was extracted using the "calculate geometry" function.

(CuiYangCui, Yang & Chen, 2003; LiuMiaoLiu, Miao & Tian, 2017; Xu, 2016).

381

382

383

384

385

386

387

Commentato [MR14]: Which GPM product hab been uses at which resolution? Except for the DEM in table 2 information on spatial and temporal resolution and scale of input data is missing. Please add this information in table. Due to this, the analysis of input data scale and resolution issues and their possible impact on the results in the discussion is completely missing, but this can add interesting prspectives to the model. Please consider to discuss this elements in the manuscript

slope, and is extremely prone to cause causing debris flows (Pan et al., 2012; Tan Yang Tan, Yang & Shi, 1990; Zhang & Guo, 2021). To address the effect of rainfall, we chose selected three factors to characterize the triggering effect of heavy rainfall on debris flows in 2020₇: the number of heavy rainstorms, the number of rainstorms, and the number of heavy rains. Based on the distinctive interannual variation variability in precipitation distribution in the study area between dry and rainy seasons, we chose the average rainfall during the rainy season (April to September) to characterize the effect of early antecedent precipitation on nurturing developing debris flows. Therefore, a total of 183 daily precipitation data were extracted for dates from 2020/04/01 to 2020/09/30 in the study area had been extracted, and the field calculator and the regional statistical function of ArcMap had been was used to calculate the average rainfall offor the 2020 rainy season for each watershed unit. Using ArcMap's model builder, a total of 366 daily precipitation data infor 2020 were sequentially screened for the number of heavy rainstorms with a cumulative daily precipitation of 100-250-100 mm, the number of rainstorms of with 50-100 mm-50 mm, and the number of heavy rains of 50 mm-25-50 mm, and; then using the field ealeulator to add up, we summed the number of days in compliance with the raster cells, and finally using ArcMap function of zonal statistics as table to calculate using the field calculator, and calculated the average number of heavy rainstorms, the average number of rainstorms, and the average number of heavy rainfall for each watershed unit with the ArcMap function of zonal statistics table.

(3) Geological conditions. Fracture zones affect the continuity and stability of rocky soil, meanwhile, the and surface soil provides a rich sediment source for debris flows (*Pham et al.*, 2016). Consequently, we used fracture zone density and soil texture to characterize the influence of geological conditions on debris flows. Fracture zone density was calculated by dividing the length of the fracture zone in each watershed unit by the watershed area. Soil texture was calculated separately for using the average content of clay, silt, and sand within the watershed unit using and the function of zonal statistics as table.

Vegetation conditions. The roots of plants have the function of fixing the rock and soil mass, and helping to improve soil erosion resistance (*Huang et al.*, 2022). To some extent, it inhibits erosion and hinders the sliding of the topsoil (*ZhaoWu & Wang*, 2006). Therefore, we used ArcMap function of zonal statistics as table to calculate the average Normalized Difference Vegetation Index of each watershed unit to characterize vegetation cover.

(4) Vegetation conditions. Plant roots stabilize the rock and soil mass, and increase soil resistance to erosion (*Huang et al.*, 2022). To some extent, plant roots inhibit erosion and hinder the sliding of the topsoil (*Zhao, Wu & Wang*, 2006). We used the ArcMap function of zonal

statistics to calculate the average Normalized Difference Vegetation Index of each watershed unit to characterize vegetation cover.

(5) Human activities. The geological Geological structure and surface become unstable under the efforts of with land use change. Meanwhile, a great deal of generatedchanges, which also generate loose deposit provides deposits providing material sources for debris flows (Huang et al., 2022; Tien Bui et al., 2017; Xu, 2016). Road transportation is the harbinger of social production, road network construction could be an indication of the an indicate regional land development intensity to a great extent. Thereout, The. We used the ArcMap function of zonal statistics as table was used to calculate the land use typetypes with the largest proportion of proportions for each watershed unit. Highway Densities of highway density, railway density, density of urban primary roads, density of urban secondary roads, density of urban tertiary roads, density of urban quaternary roads, density of and county and town roads were calculated using highway length, railway length, urban primary roads length, urban secondary roads length, urban tertiary roads length, and urban quaternary roads length, corresponding road type lengths divided by the watershed area, respectively.

Table 2: Selected evaluation factors and their data sources.

3.2.3 Data pre-processing

Due to We used the presence of Random Forest (RF) model to reduce the noise, which impairs in the data qualitysets and model performance, The literature to select evaluation factors following the approach of (Kursa & Rudnicki, 2011) has demonstrated that preprocessing data with the Random Forest (RF) model is a reliable and effective approach. Therefore, we employ this approach to select the evaluation factors.

Firstly.

First, a RF model was built with all the evaluation factors in Python. Secondly after digitizing, data formatting, and unifying georeferencing. Second, the model was trained again using the GridSearchCV module, which iterates through all permutations of incoming parameters to find the best hyperparameter. Thirdly, the contributionThird, contributions of the evaluation factors waswere obtained and ranked. Finally, we filtered out the evaluation factors, were filtered. Through analyzing the initial factors and their contribution in Table 13, we founddetermined that the contribution of six6 factors, namely railway density, highway density, the density of urban primary roads, the density of urban secondary roads, the density of urban tertiary roads, the density of urban quaternary roads, were all-less than 0.01%%, and they apparently did not in the same order of magnitude as other factors. Therefore, we considered these six6 factors as noisy data and removed them. Eventually, the From further evaluation indicators. The remaining

ha formattato: Tipo di carattere: Grassetto

Formattato: Allineato al centro, Rientro: Prima riga: 0 car

Commentato [MR15]: All the software/modules mentioned should be cited and referenced. This is particularly relevant for the free and open source software and modules which are provided for free to the users.

evaluation factors are shown in Fig. 25.

Fig. 25: Processed factors affecting debris flows susceptibility.

(a) Relative elevation difference. (b) Average slope. (c) Watershed area. (d) Average rainfall during the rainy season. (e) Number of heavy rainstorms. (f) Number of rainstorms. (g) Number of heavy rains. (h) Fracture zone density. (i) Sand content. (j) Silt content. (k) Clay content. (l) NDVI. (m) Land use. (n) Density of county and town roads.

Table 43: Contribution of evaluation factors before and after pre-processing.

Data annotation. We chose 274 historical debris flows that occurred in YNR Basin up until 2019 to mark(1) Data annotation. The debris flow inventory was derived from the nationwide geohazard census done by the Resource and Environment Science and Data Center (www.resdc.cn/). After data verification with local histories, books, reports, statistic data, relevant field surveys, and related literature, a total of 274 debris flow hazards in the study area were found as of the end of 2019, and the attribute information included the field number, geographic location, damage, groundwater grade, and the current degree of stability, and so on. We used this inventory to annotate each watershed unit. Those units that had experienced debris flows were assigned a label of '1', while those that had not were assigned a label of '0'. The entire set of watershed units was subsequently divided into two groups, namely of 'debris flow' and 'no debris flow',

(2) Data sampling. In order to To prevent sample imbalance from affecting model accuracy, we employedused the synthetic minority oversampling technique (SMOTE) to balance the sample size, which analyzed a small number of samplesdata and added simulated new samplesdata to the dataset (WuYang & Niu, 2020; ZJ & Yu, 2022). when needed (Wu, Yang & Niu, 2020; ZJ & Yu, 2022). Eventually, the watershed units unit ratio with 'debris flow' to those with 'no debris flow' was 1:1, and the total sample size was 2140 items.

Data division. The whole dataset has been divided into two subsets with a ratio of 7:3 for DFS model training and testing (*Huang et al.*, 2022)(3) Datasets division. The whole dataset was divided into two subsets of 7 to 3 for DFS model training and testing, respectively (*Huang et al.*, 2022).

Experiments and analysis of results

4.1 Model construction

The RF and SVM models were trained by using the scikit-learn library within Python, which integrates various machine-learning methods. FirstlyFirst, RF was generated using the Random Forest Classifier method, and Linear SVM and RBFSVM were generated using the SVC method.

ha formattato: Evidenziato

Commentato [MR16]: Do you mean 70 and 30%?

Secondly Second, we then adjusted the hyperparameters, taking into account the relationship between model complexity and generalization error, to minimize the generalization error and improve the accuracy and generalization ability of the model (Duan et al., 2022). Based on the effect of each hyperparameter on the model complexity, the RF model was adjusted in the order of the number of classifiers, the maximum depth, the minimum number of samples of the leaf nodes, the condition limiting the continuation of the subtree division, the maximum number of features, and the decision tree algorithm. Specifically, we employed the ten-fold cross-validation method to generate learning curves for each hyperparameter within a large interval. Once we determined the range of subintervals with the highest accuracy, we used the grid search method to determine the optimal values. Ultimately, the optimal hyperparameters for the RF model were 91, 21, 1, 2 and 11 corresponding to the number of classifiers, the maximum depth, the minimum number of samples of the leaf nodes, the condition limiting the continuation of the subtree division, and the maximum number of features, respectively. As the SVM model had fewer hyperparameters, we adjusted it only using the grid search method. The optimal penalty parameter C of 1search range and hyperparameter values for each model are shown in Linear SVM and 5 in RBFSVM. In addition, the dimensionality parameter Gamma in RBFSVM of 0.05 Table 4.

After the above processes, the susceptibility evaluation Table 4: Hyperparameter values for each model.

DFS models for the YNR Basin were developed based on the optimal hyperparameters for the RF, Linear SVM, and RBFSVM methods, respectively. In response to the characteristics of alpine-valley areas with distinct wet and dry conditions and complex debris flow genesis in the context of geographic big data, and based on the applicability of the RF and the SVM models in dealing with high-dimensional, non-linear data, the model usesused average rainfall during the rainy season to assess the impact of rainfall on debris flow, and usesused RF and SVM to quantitatively assess the drivers and study area susceptibility.

4.2 Analysis of results

489

490

491

492

493

494

495

496

497

498

499

500

501

502

503

504

505

506

507

508

509

510

511

512

513

514

515

516

517

518

519

520

521

4.2.1 Analysis of the pre-processing results

The AUC of the RF model on theusing test data improved increased from 0.73 to 0.97. The ROC curve was closer to the upper left corner as shown in (Fig. 3. In addition, the6). Further, model training time was reduceddecreased by 23%, from 105 seconds to 84 seconds.

Fig. 36: ROC curves.

Data preprocessing eliminated the impact of redundant data on the model and on the

Commentato [MR17]: What do you mean for "adjusted"?

Commentato [MR18]: What do you mean for "adjusted"?

remaining evaluation factors, so the contribution rate of the remaining evaluation factors has changed. The total contribution rate of such as topographic conditions, human activities, and vegetation conditions increased by 0.068, 0.065, and 0.017, respectively. While, while those of rainfall conditions and geological conditions decreased by 0.115 and 0.035, respectively (Fig. 47). In addition, the contribution rate of the most important evaluation indicator (relative elevation difference) increased by 0.09 (Table 43).

Fig. 47: The contribution rate of the five main categories of evaluation factors before and after pre-processing.

4.2.2 Analysis of evaluation factors

Experimental results <u>presented indicated</u> that topographic conditions <u>arewere</u> the decisive factors during the formation of debris flow in the YNR Basin, and geological conditions, rainfall conditions, human activities, and vegetation conditions <u>arewere</u> important factors, with contribution rate corresponding to 0.425, 0.195, 0.173, 0.133, and 0.074 (Fig. 47), respectively. The top 3 factors are explanatory conditions were topographic, geological, and rainfall <u>conditions</u>.

In terms of the 14 evaluation factors, the The relative elevation difference (contribution rate: 0.274) iswas the most vitalimportant evaluation indicator and playswith a key role in the formation of debris flows. This iswas followed by watershed area, NDVI, and density of county and town roads ranking third3rd and fourth4th, respectively. The rest factors areothers were in the order of average slope, average rainfall during the rainy season, land use, sand content, silt content, clay content, the number of heavy rainstorms, fracture zone density, and the number of heavy rains. The number of rainstorms is found to have had a relatively small lesser impact on the formation of debris flows (Fig. 58).

Fig. 5: Contribution rate8: The contribution of evaluation factors to the total variability in debris flow formation.

4.2.3 Model accuracy analysis

The evaluation results of the <u>RF</u> model effectiveness indicate that <u>RF hashad</u> higher <u>values of</u>

Accuracy, Precision, Recall, F1-score, and Kappa (Table 25), and theits ROC curve of RF

convergesconverged faster than that of RBFSVM and Linear SVM (Fig. 6). It means 9). This

indicated that the RF model enables a comprehensive RF was most suitable of the three models

for examination of the spatial correlation between historical debris flows and elevation factors,
improving the assessment accuracy of DFS.

Table 25: Comparison of model accuracy.

Fig. 69: The ROC curves.

Commentato [MR19]: Why? Can be this possibilty related with the sampling strategy adopted in the study?

4.2.4 Susceptibility analysis

According to the evaluation criterion, there is a positive correlation between the susceptibility Susceptibility class and the density distribution of debris flows, were positively correlated with a higher density of debris flows leading to higher susceptibility classes. The difference in density between very high and very low susceptibility zones serves as an indicator of the predictive performance of the model (*Li et al.*, 2022)(*Li et al.*, 2022). The experimental Our results presents howed that the prediction performance of the RF iswas better than the that of RBFSVM, and the while that of Linear SVM iswas the worstlowest (Fig. 7). While all 10).

All three models demonstrated an increase in debris flow density with increasing susceptibility class, but the difference in debris flow density between the very high and very low susceptibility zones iswas greatest for the RF model, with 47 debris flows per 1000 km², followed by RBFSVM with 37 debris flows per 1000 km², and the lowest for Linear SVM with 11 debris flows per 1000 km². These results indicated that the RF model iswas more adept at discriminating very high and heigh susceptibility zones and exhibits exhibited superior predictive performance when compared to the other two models.

Fig. 710: Density of debris flows in each of the three models' susceptibility zones of the three models.

Fig. 811: Susceptibility zoning in the upstream section of the YNR Basin. (a) RF model. (b) RBF SVM model. (c) Linear SVM model.

Based on the analysis of historical debris flows and the overlap in susceptibility zones overlapping (Fig. 8), the 11), we determined that RF and RBFSVM are more reasonable for modellingmodelled susceptibility zones in the YNR Basin better than the Linear SVM in YNR Basin. The Linear SVM predicted many of the very high and high susceptibility zones which havehad no historical debris flow distribution, flows, therefore the credibility of its predictions iswas low. The high dimensionality of debris flow data may be a contributing factor, as Linear SVM had difficulty effectively capturing the complex nonlinear relationships in the dataset. This resulted in tendency to overfit the training data, reducing its accuracy in predicting susceptibility to debris flow hazards. The Kappa value of the Linear SVM model was only 0.37 (Table 5), indicating that the model was unable to make consistent predictions at different conditions or times, indirectly confirming the existence of the overfitting problem. This instability limits the applicability of the model to DFS prediction.

The results of the RF's DFS elassification spatial distribution map showobtained with RF showed that the very high susceptibility zones in the upstream section of the YNR Basin arewere mainly distributed along the mainstream of the Nujiang River. The dominant factors arewere

Commentato [MR20]: This analysis maybe more effective using proportions/density along Y axis, rather than number/counts. Please consider to use prediction/success rate curves by Chung and Fabbri 2003, which express similar evaluations

Formattato: Rientro: Prima riga: 0,74 cm

Commentato [MR21]: Why? Can you exclude that this depends primarily on how you have applied/trained the model?

topographic and geological conditions in the very high susceptibility zones of Gongshan, Fugong, and Lushui counties due to the associated with active neotectonic movements resulting in the development of numerous bulge structures and compressional folds. The swiftly flowing water, driven by the effects of tectonic activity and fluvial erosion, results in the formation of steep riverbanks. After the Holocene, the bulge of the mountains and the deepening of the river valleys had led to the formation of alpine-valley landscapes. Furthermore, the deep and large fractures of the Nujiang River, along with numerous tectonic fractures and joint fissures, control the geomorphological development in the area, leading to extremely developing gravity geomorphology, including debris flow extreme gravity geomorphology, including debris flows(Liu & Tang, 1995; Tang & Zhu, 2003).

Fig. 912: Susceptibility zoning in the downstream section of the YNR Basin. (a) RF model. (b) RBF SVM model. (c) Linear SVM model.

Based on The RF model performed more robustly for susceptibility zoning in the YNR Basin (Fig. 12), as shown by the overlap between historical debris flows and susceptibility areas, as well as and by the analysis of model accuracy (Fig. 9), the RF model performs more robustly for susceptibility zoning in YNR Basin. The modeling resultresults of RBFSVM showshowed an overall higher susceptibility than the actual situation. Compared to the predicted result of the Linear SVM model and that indicated by historical debris flow data, we find that. In the Linear SVM, many historical debris flow areas arewere distributed in very low and low susceptibility areaszones and few historical debris flowsflow areas arewere distributed in some high susceptibility areaszones, which makes the rendered predictions less reliable. Accordingly, lead to overfitting of the training data, and resulted in lower accuracy in predicting the susceptibility to debris flow disasters.

Consequently, the RF model was used for susceptibility zoning in the downstream section of the YNR Basin, the The results revealedshowed that areas with very high and high susceptibility to debris flows are predominantlywere concentrated in northern Longling County, northern Longyang District, eastern and southeastern Zhenkang County, eastern Shidian County, and central Yongde County, and debris flowthose of susceptibility probability is aboutresponse to 0.86, 0.85, 0.84, and 0.81, respectively.

Conclusion

Taking the Yunnan section of the Nujiang River (YNR) Basin as a case study, this article discussed the performance of three popular supervised machine learning algorithms in analyzing debris flow susceptibility in the alpine valley area throughout a data driven perspective. And the results indicate that the RF model outperforms both the RBFSVM model and Linear SVM model

in terms of accuracy of prediction results, and prediction performance. It implies that the RF model is more suitable for susceptibility assessing of debris flow in YNR Basin.

Based on the contribution rate of the evaluation factors generated by the RF model, topographic conditions are the decisive factor in the formation of debris flows in YNR Basin. Geological conditions, rainfall conditions, human activities, and vegetation conditions are essential to forming debris flows. In addition, among the 20 evaluation factors, the relative elevation difference plays a vital role in the formation and occurrence of debris flows in our study area.

The results of the RF-based DFS classification spatial distribution map indicate that the very high susceptibility zones are mainly distributed along the mainstream of the Nujiang River in the study area. Very high susceptibility zones are primarily situated in Gongshan County, Fugong County, Lushui County, northern Longling County, northern Longyang District, eastern and southeastern Zhenkang County, eastern Shidian County, and central Yongde County where the terrain and geological conditions are extremely conducive to the development of gravity geomorphy.

Discussion

623

624

625

626

627

628

629

630

631

632

633

634

635

636

637

638

639

640

641

642

643 644

645

646

647

648

649

650

651

652

653

654

655

656

This study further demonstrates the demonstrated applicability of the RF model to assess DFS. (1) In terms of model accuracy, the in the YNR Basin. The RF model exhibits exhibited a comparable AUC to the research results utilizing that obtained with the Backpropagation Neural Network and hashad higher Accuracy and a greater overlap between the predicted very high and high susceptibility zones and historical debris flows (Wang et al., 2010). In addition, the difference in AUC, very high and very low susceptibility zone debris flow density for the RF model are all outperformance of outperformed the deterministic coefficient model (Li Yang & Wei, 2019)(Li, Yang & Wei, 2019). (2) In terms of methodology, Further, the methods in the RF model does do not rely on expert experience, making it more objective and scientificaccurate than the numerical division of the sensitivity of each factor (Tang, 2005) and the method of assigning different weights to each factor (Tang, 2005). (3) In terms of prediction results, this work further validates the research inferences of Tang and Li from the perspective of more detailed results (LiYang & Wei, 2019; Tang, 2005). Nevertheless, based on the overlap between historical debris flows and susceptibility zones, and the analysis of model accuracy, the distribution of very high and high susceptibility zones in the study is more similar to historical debris flows and has a higher AUC compared with research inferences of Tang and Li (LiYang & Wei, 2019; Tang, 2005), making the results of the susceptibility zones in this study more reliable. (4) the conclusions of the Nujiang River basin by Xu and Guo We also further validated the inferences of Tang and Li and others

regarding more detailed results (*Li*, Yang & Wei, 2019; Tang, 2005). Nevertheless, the distribution of very high and high susceptibility zones in this study aligned with historical debris flows better and had a higher AUC than that exhibited in the study of Li and Tang (*Li*, Yang & Wei, 2019; Tang, 2005), indicating a higher reliability of susceptibility zone prediction in this study. Finally, Guo and Xu (GuoLuoGuo, Luo & Tang, 2015; Xu, 2016) showed that topography, source of debris flow, and rainfall arewere the three main conditions for forming debris flows, which coincide with in Nujiang River Basin, reflecting the results ranking of debris-flow contributing factors in this study in terms of contribution ranking.

The dataData pre-processing based on the contribution rate of evaluation-factors generated by the RF model iswas reliable. Multicollinearity has relatively little influence on rarely influences the proposed model, due to a large number of training samples. Thus, we used the RF to deal with the reduce noise, which has had a great effect on the accuracy of the model, and the accuracy iswas significantly improved. The reason This is that possible because nodes of this the RF model are randomly selected with equal probability to construct decision trees; the evaluation factors with a lower contribution may negatively affect the model performance and increase generalization error (Rogers & Gunn, 2006). Furthermore, this the proposed model measures the importance of the evaluation factors not exclusively in terms of their contribution to the predicted results, but rather in terms of their ability to contribute to predicted results in this proposed model rather than exclusively in terms of their contribution to the predicted results (Zhang et al., 2019). In addition, the increased higher AUC and the a better-performing ROC curve after data preprocessing of the model further validate that taking the RF to deal with the eliminating noise is reliable with RF leads to more accurate results.

The prePre-processing removed six6 evaluation indicators, but it does not mean that they do not influence the formation of debris flows. As variables. Variables with a higher number of categories in the RF will tend to higher contribution, contribute more; 80% of the existing roads in the study area are roads below Class IV, and with; the relatively few railways, highways, urban quaternary roads, urban tertiary roads, urban secondary roads, and urban primary roads, resulting result in thea low number of categories for these six6 evaluation factors. To address this the issue, the next step we will be to explore the impact of railways, highways, and urban roads, on debris flow using more rational characterizations or adding weights to find out the impact of road construction on debris flows. What's more Additionally, the number of rainstorms data are in the dataset was relatively sparse, resulting in small information gain during decision tree generation.

Thus, its contribution is low. As a consequence Consequently, future research will cluster include clustering of indicators of the number of heavy rains, number of rainstorms, and number of heavy

Commentato [MR22]: What does this mean? Have you done this or this expresses a "willingness to do" for the future? If the second case please remove and simply aknowledge the importance of this issue.

Commentato [MR23]: Can be this related to the type and resolution of input data are you considering?

rainstorms, and perform spatial correlation analysis to reveal the impact differences in effects caused by the uneven distribution of rainstorms during the rainy season in the study area.

The elevation factors of debris flows perform dissimilar effects under the different study scales. At the study Model applicability. (1) The RF and RBFSVM models are well suited to DFS assessments which require high-dimensional data; in addition, related literature shows that they have higher accuracy in landslide, flood, and other disaster susceptibility assessments than other models (Fang et al., 2022; Prasad et al., 2022). The Linear SVM model cannot capture complex nonlinear relationships well and is prone to overfitting, thus not applicable to DFS assessment. In this study, the Linear SVM model predicted many zones with very high and high debris flow susceptibility but without historical debris flow distribution, therefore, its prediction credibility was low. (2) The RF and RBFSVM models have some limitations. Training the RBFSVM model with high-dimensional data is time-consuming, sensitive to noise and outliers, and demands meticulous data cleaning and filtering. Additionally, predictions of the RBFSVM, relying on nonlinear mapping, are relatively challenging to interpret. On the other hand, the RF model tends to favor lower contributions when presented with sparse data. Six evaluation indicators were removed in the preprocessing portion of this study, but they may, in fact, contribute to the formation of debris flow; The results of the quantitative ranking of factor contributions to DFS in the study area need to be investigated further. (3) This study clarifies the applicability, accuracy, and limitations of the three models, providing researchers with methodological references and directions for model improvement; in addition, it provides scientific basis for disaster prevention and avoidance in the alpine-valley area.

Elevation factors of debris flows had dissimilar effects at different scales. At the scale of the Yunnan section of the Nujiang River Basin, the major evaluation factors for debris flows arewere topographic, geological, and rainfall conditions. However, when scaled down to the scale of each county, the main evaluation factors may change when scaled down to each county (ChengYu & L; , 2010). Through scientific literature search, it was discovered that precipitation significantly impacts Longling County, Zhenkang County, Shidian County, and Yongde County(Cheng, Yu & Chang, 2010). Thus, precipitation significantly impacts Longling, Zhenkang, Shidian, and Yongde Counties, resulting in an increased likelihood of debris flows, floods, and other disasters. Longling County, Longyang District, and Zhenkang County experience extensive human activities, including construction projects such as for water conservancy conservation, road construction, mining, and logging, leading to severe soil erosion. The geological environment Geology also plays a crucial role insignificantly affects these areas, such as Longling County, which features a large number of fractures on the eastern side of Chongshan, and;

Zhenkang County has fractures and folds in varying directions contributing to a complex and variable geological structure. In addition, Yongde County has a high concentration of mudstones, sandstones, and slatesslate with looser textures and more developed joint fissures. The analysis (Cheng et al., 2000; Hou et al., 2005; Wu, Li & Qian, 1993; Xiao & Wu, 1992; Zhang & Li, 1997). Analysis of the drivingevaluation factors of debris flows must be tailored to different regional scales in complex terrain areas.

This study provides tested the underlying techniques of the model for evaluating the susceptibility of alpine-valley-typeareas to debris flows, which has certain promotion and an application value for the similar researches on research at watershed scales. However, there are some limitations that need to be further improved. FirstlyFirst, we did not consider the temporal distribution of debris flows in the model due to insufficient statistical data. Treating debris flows occurring at different times as a type of marker sample would affect the accuracy of the cause analysis of debris flows (Huang et al., 2022)(Huang et al., 2022). SecondlySecond, the assessment of the strengths and weaknesses of the predictions was based on the assumption that the higher the susceptibility class and the higher the density of debris flow distribution (Li et al., 2022) are correlated (Li et al., 2022). If extensive Extensive field research could be combined in future studies, combined with modeling will significantly improve reliability of the results may be.

Conclusions

Data acquisition for debris susceptibility assessments in the Yunnan section of the Nujiang River (YNR) Basin is challenging; the predominant use of traditional debris flow susceptibility assessment methods results in low accuracy that fails to fulfill practical needs. Here, we addressed these issues with systematical collection and processing of relevant debris flow data, including an analysis of the performance of three machine learning algorithms in analyzing debris flow susceptibility in the alpine-valley area. The results indicated that the RF model outperforms both the RBFSVM and the Linear SVM models in terms of accuracy and precision of prediction indicating that the RF model is more convincing.

suitable for susceptibility assessment of debris flow in the YNR Basin. This study provides valuable methodological analysis and directions for improvement of the model.

The contribution rate of the evaluation factors generated by the RF model showed that topographic conditions were the decisive factor in the formation of debris flows in the YNR Basin. Geology, rainfall conditions, human activities, and vegetation conditions are essential to forming debris flows. In addition, the relative elevation difference was vital among the 20 evaluation factors in the formation and occurrence of debris flows in our study area.

759 The results of the RF-based DFS classification distribution map indicated that the very high 760 susceptibility zones are mainly distributed along the mainstream of the Nujiang River. Very high 761 susceptibility zones are primarily situated in Gongshan County, Fugong County, Lushui County, 762 northern Longling County, northern Longyang District, eastern and southeastern Zhenkang 763 County, eastern Shidian County, and central Yongde County where the terrain and geological 764 conditions are extremely conducive to the development of gravity geomorphology. These results 765 support efforts in implementing more targeted preventive measures in very high and high 766 susceptibility zones, significantly enhancing overall preparedness for debris flows. 767 768 References 769 Bao YD, Chen JP, Sun XH, Han XD, Li YC, Zhang YW, Gu FF, and Wang JQ. 2019. Debris flow 770 prediction and prevention in reservoir area based on finite volume type shallow-water 771 model: a case study of pumped storage hydroelectric power station site in Yi County, 772 Hebei, China. Environ Earth Sci 78:1-16. 10.1007/s12665-019-8586-4 773 Breiman. 2001. Random forests. MACH LEARN 45(1):5-32. Formattato: Giustificato 774 Chang KT, Merghadi A, Yunus AP, Pham BT, and Dou J. 2019. Evaluating scale effects of 775 topographic variables in landslide susceptibility models using GIS-based machine 776 learning techniques. Sci Rep 9:12296. 10.1038/s41598-019-48773-2 777 Cheng JMJ, Yu H, and Chang L: C. 2010. Study on assessment of multi-scales mine geological Formattato: Giustificato 778 environment—a case study baibeatifyingne in xinjiang. *Xinjiang Geol*:346-349. 779 Cheng JD, Zhang ZC, He DX, and Zhang ZY. 2000. Longling County Chronicles. Beijing: 780 Publishing House of China. 781 Cui P, Yang K, and Chen J. 2003. Relationship Between Occurrence of Debris Flow and Antecedents Formattato: Giustificato 782 Precipitation: Taking the Jiangjia Gully as An Example. Sci Soil Water Conserv 1:11-15. 783 10.16843/j.sswc.2003.01.006 784 Dou J, Yunus AP, Tien Bui D, Sahana M, Chen CW, Zhu ZF, Wang WD, and Pham BT. 2019. 785 Evaluating GIS-based multiple statistical models and data mining for earthquake and 786 rainfall-induced landslide susceptibility using the LiDAR DEM. Remote Sens 11:638. 787 10.3390/rs11060638 788 Duan XY, Li YY, Linghu YX, and Hu RL. 2022. Research on the Method of Side Channel Attack* Formattato: Giustificato 789 Based on RF Algorithm. Netinfo Security. 790 Fang Z, Wang Y, Duan H, Niu R, and Peng L. 2022. Comparison of general kernel, multiple kernel, 791 infinite ensemble and semi-supervised support vector machines for landslide susceptibility 792 prediction. Stochastic Environmental Research Risk Assessment 36:3535-3556. 793 Guo RFR, Luo Y, and Tang S. 2015. Analysis on the causes of mudslides in Fugong on May 10, Formattato: Giustificato 794 2014. Journal of Catastrophology 30:102-107.

Hou XH, Du SL, Ding XH, and Ma YM. 2005. Nujiang Lisu Autonomous Prefecture Chronicles.

796	Beijing: Publishing House of Minority Nationalities.	
797	Huang H, Wang YS, Li YM, Zhou Y, and Zeng ZQ. 2022. Debris-Flow Susceptibility Assessment	Formattato: Giustificato
798	in China: A Comparison between Traditional Statistical and Machine Learning Methods.	
799	Remote Sens 14:4475. 10.3390/rs14184475	
800	Huang JC, Li X, Zhang LY, Li YB, and Wang PJ. 2020a. Risk perception and management of debris	
801	flow hazards in the upper salween valley region: Implications for disaster risk reduction in	
802	marginalized mountain communities. Int J Disaster Risk Reduct 51:101856.	
803	10.1016/j.ijdrr.2020.101856	
804	Huang JC, Xu HJ, Duan XW, Li X, and Wang PJ. 2020b. Activity patterns and controlling factors	
805	of debris flows in the Upper Salween Alpine Valley. Nat Hazards 103:1367-1383.	
806	10.1007/s11069-020-04039-z	
807	Janizadeh S, Avand M, Jaafari A, Phong TV, Bayat M, Ahmadisharaf E, Prakash I, Pham BT, and	
808	Lee SJS. 2019. Prediction Success of Machine Learning Methods for Flash Flood	
809	Susceptibility Mapping in the Tafresh Watershed, Iran. 11.	
810	Kursa MB, and Rudnicki WR. 2011. The all relevant feature selection using random forest. Artif	Formattato: Giustificato
811	Intell. 10.48550/arXiv.1106.5112	
812	Lana JC, Castro PdTA, and Lana CE. 2022. Assessing gully erosion susceptibility and its	
813	conditioning factors in southeastern Brazil using machine learning algorithms and	
814	bivariate statistical methods: A regional approach. Geomorph 402:108159.	
815	10.1016/j.geomorph.2022.108159	
816	Li K, Zhao JSJ, Lin YLY, and Zhou B. 2022. Assessment of debris flow susceptibility based on ◆	Formattato: Giustificato
817	different slope unit division methods and BP neural network. Bull Surv Mapp:68.	
818	Li <u>YMY</u> , Yang L, and Wei <u>SHS</u> . 2019. Susceptibility assessment of debris flow in Nujiang befecture	
819	based on the catchment. Resour Environ Resources Environment in the Yangtze Basin	
820	28:2419-2428.	
821	Li YY, Wang HG, Chen JP, and Shang YJ. 2017. Debris flow susceptibility assessment in the	
822	Wudongde dam area, China based on rock engineering system and fuzzy C means	
823	algorithm. Water 9:669. 10.3390/w9090669	
824	Liang Z, Wang CM, Zhang ZM, and Khan K-U-J. 2020. A comparison of statistical and machine-	Formattato: Giustificato
825	learning methods for debris flow susceptibility mapping. Stochastic Environmental	
826	Research Risk Assessment 34:1887-1907. 10.1007/s00477-020-01851-8	
827	Lin HT, and Lin CJ. 2003. A Study on Sigmoid Kernels for SVM and the Training of non-PSD	
828	Kernels by SMO-type Methods. Neural Comput.	
829	Liou Y A, Nguyen AK, and Li M-H. 2017. Assessing spatiotemporal eco-environmental	
830	vulnerability by Landsat data. Ecolog Indic 80:52-65. 10.1016/j.ecolind.2017.04.055	
831	Liu XL, Miao C, and Tian CS. 2017. Comparative Analysis of Two Methods for Assessing Hazard	Formattato: Giustificato
832	of Landslide and Debris-flow on a Regional Scale. J Disaster Prev Mitig Eng 37:8.	
833	10.13409/j.cnki.jdpme.2017.01.010	
834	Liu XL, and Tang C. 1995. Debris Flow Hazard Assessment. Beijing: Science Press.	

835	Liu XY. 2017. Hydrological and Water Resources Study of the Nujiang River Basin. Beijing: China	
836	Water&Power Press.	
837	Liu YY, Di BF, C.A. S, and Zhan Y. 2018. Debris Flows Susceptibility Assessment in Wenchuan	
838	Earthquake Areas Based on Random Forest Algorithm Model. <i>Mountain Research</i> .	
839	10.16089/j.cnki.1008-2786.000372	
840	Luo W, and Liu C. 2018. Innovative landslide susceptibility mapping supported by geomorphon	
841	and geographical detector methods. Landslides 15:465-474. 10.1007/s10346-017-0893-9	
842	Luo YH. 2009. Research on Geologic Environment in Three Parallel Rivers Region Doctor. China	Formattato: Giustificato
843	University of Geosciences.	
844	Ma WL. 1999. Hydrogeological Survey Report of Northwest Yunnan (1:50,000 scale). Yunnan	
845	Bureau of Geology and Mineral Resources.	
846	Min Y, Hu J, Li C, Xu YJ, Li HH, Li X, Wan SY, Li L, and Yang SY. 2013. Prediction Model about	
847	Landslide and Debris Flow in Yunnan Province. <i>Journal of Catastrophology</i> 28:216-220.	
848	CNKI:SUN:ZHXU.0.2013-04-042	
849	Ming Q. 2006a. The Landoform Development and Environment Effects of Three Parallel Rivers	
850	in the North of Longitudinal Range-Gorge Region(LRGR). Lanzhou University in	
851	Lanzhou, China.	
852	Ming QZ. 2006b. The Landform Development and Environment Effects in the area of Three	
853	Parallel Rivers, Northern Longitudinal Range-Gorge Region (LRGR) Doctor. Lanzhou	
854	University.	
855	Oh HJ, and Lee S. 2017. Shallow landslide susceptibility modeling using the data mining models	
856	artificial neural network and boosted tree. Appl Sci 7:1000. 10.3390/app7101000	
857	Pan HL, Ou GQ, Huang JC, and Cao B. 2012. Study of rainfall threshold of debris flow forewarning	Formattato: Giustificato
858	in data lack areas. Rock Soil Mech 33:5. 10.19630/j.cnki.tdkc.2014.02.025	
859	Pham BT, Tien Bui D, Prakash I, and Dholakia M. 2016. Rotation forest fuzzy rule-based classifier	
860	ensemble for spatial prediction of landslides using GIS. <i>Nat Hazards</i> 83:97-127.	
861	10.1007/s11069-016-2304-2	
862	Prasad P, Loveson VJ, Das B, and Kotha M. 2022. Novel ensemble machine learning models in	
863	flood susceptibility mapping. Geocarto International 37:4571-4593.	
864	Qiang Z, Peng C, Jing HC, Yu LA, and Sl C. 2019. Regional risk assessment of debris flows in	Formattato: Giustificato
865	China—An HRU-based approach. Geomorph 340:84-102.	
866	10.1016/j.geomorph.2019.04.027	
867	Reichenbach P, Rossi M, Malamud BD, Mihir M, and Guzzetti F. 2018. A review of statistically-	
868	based landslide susceptibility models. Earth Sci Rev 180:60-91.	
869	10.1016/j.earscirev.2018.03.001	
870	Rogers J, and Gunn S. 2006. Identifying feature relevance using a random forest. Subspace, Latent	Formattato: Giustificato
871	Structure and Feature Selection: Statistical and Optimization Perspectives Workshop,	
872 873	SLSFS 2005, Bohinj, Slovenia, February 23-25, 2005, Revised Selected Papers: Springer.	
×/-	n 173-184	

p 173-184.

874	Sujatha ER, and Sridhar V. 2017. Mapping debris flow susceptibility using analytical network	
875	process in Kodaikkanal Hills, Tamil Nadu (India). Journal of Earth System Science 126:1-	
876	18.	
877	Sun JB, Qin SW, Qiao SS, Chen Y, Su G, Cheng QS, Zhang YQ, and Guo X. 2021. Exploring the	Formattato: Giustificato
878	impact of introducing a physical model into statistical methods on the evaluation of regional	
879	scale debris flow susceptibility. <i>Nat Hazards</i> 106:881-912. 10.1007/s11069-020-04498-4	
880	Suykens J, and Vandewalle J. 1999. Least Squares Support Vector Machine Classifiers. Neural	
881	Process Lett 9:293-300. 10.1016/j.csda.2013.09.015	
882	Tan B, Yang DW, and Shi SG. 1990. The study of prediction for debris flow caused by rainstorm.	
883	J China Railway Soc:14-20.	
884	Tang C. 2005. Susceptibility spatial analysis of debris flows in the Nujiang River Basin of Yunnan.	
885	GeoScience 24:178-185.	
886	Tang C, and Zhu J. 2003. Research on Landslides and Debris Flows in Yunnan. Beijing: The	
887	Commercial Press.	
888	Tien Bui D, Tuan TA, Hoang N-D, Thanh NQ, Nguyen DB, Van Liem N, and Pradhan B. 2017.	
889	Spatial prediction of rainfall-induced landslides for the Lao Cai area (Vietnam) using a	
890	hybrid intelligent approach of least squares support vector machines inference model and	
891	artificial bee colony optimization. Landslides 14:447-458. 10.1007/s10346-016-0711-9	
892	Wang X, Zhao K, Jiang YL, and Zhu W. 2010. Study On dynamic zoning model of mud-rock flow	
893	susceptibility in Nujiang basin based on BP neural network. Ind Miner Process 51:39-	
894	43+48. 10.16283/j.cnki.hgkwyjg.2022.01.008	
895	Wu DY, Li JM, and Qian GB. 1993. Lincang County Chronicles. Kunming, Yunnan Province:	
896	Yunnan People's Publishing House.	
897	Wu XL, Yang JY, and Niu RQ. 2020. A Landslide Susceptibility Assessment Method Using	Formattato: Giustificato
898	SMOTE and Convolutional Neural Network. Geomatics and Information Science of Wuhan	
899	University 45:10. 10.13203/j.whugis20200127	
900	Xiao DH, and Wu DN. 1992. Zhenkang County Chronicles. Chengdu, Sichuang province:	
901	Publishing House of Minority Nationalities in SiChuang.	
902	Xu ⊞H. 2016. Study on Debris-flow Activity Patterns and Hazard Driving Forces of the Alpine ✓	Formattato: Giustificato
903	Vallery Area in Nujiang River Basin Master. Yunnan University.	
904	Yang YD, Tang P, Xiao HZ, and Ya XS. 2017. Preliminary Analysis on Relationships between Geo-	
905	hazards and River Systems of Yunnan Province. Journal of Catastrophology:36-39.	
906	Zhang SC, and Li GZ. 1997. Shidian County Chronicles. Beijing: Xinhua Publishing House.	
907	Zhang SH, and Wu G. 2019. Debris Flow Susceptibility and Its Reliability Based on Random Forest	Formattato: Giustificato
908	and GIS. Earth Science:20-21.	

Zhang TF, and Guo CX. 2021. Rainfall Threshold of Debris Flow in Fujian Mountainous Area,

Zhang YH, Ge TT, Tian W, and Liou Y-A. 2019. Debris flow susceptibility mapping using machine-

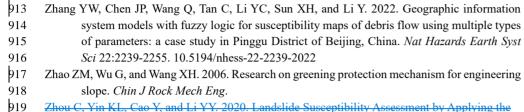
learning techniques in Shigatse area, China. Remote Sens 11:2801. 10.3390/rs11232801

China. Mountain Research 39:9.

909

910

911



Zhou C, Yin KL, Cao Y, and Li YY. 2020. Landslide Susceptibility Assessment by Applying the Coupling Method of Radial Basis Neural Network and Adaboost: A Case Study from the Three Gorges Reservoir Area. Earth Science 45:1865.

ZJ Z, and Yu Z. 2022. Flood disaster risk assessment based on random forest algorithm. *Neural*Comput Appl*:1-13. 10.1007/s00521-021-05757-6

Zou Q, Tang J, Li S, and Fan J. 2017. Susceptibility Assessment Method of Debris Flows Based on Hydrological Response Unit. *Mountain Research* 35:10. 10.16089/j.cnki.1008-2786.000247

Formattato: Giustificato